

## RESEARCH ARTICLE

10.1002/2016JG003455

## Key Points:

- Compensation day (cDOY) is the day of year when net C losses during winter are compensated by net C uptake in spring
- cDOY largely explains annual net ecosystem productivity  $NEP_c$  of forests when the site has a distinct winter respiratory loss period
- cDOY and its explanatory power depends on the integration method for annual  $NEP_c$  and on the forest type

## Supporting Information:

- Supporting Information S1

## Correspondence to:

M. Haeni,  
matthias.haeni@wsl.ch

## Citation:

Haeni, M., et al. (2017), Winter respiratory C losses provide explanatory power for net ecosystem productivity, *J. Geophys. Res. Biogeosci.*, 122, 243–260, doi:10.1002/2016JG003455.













Received 14 APR 2016

Accepted 22 DEC 2016

Accepted article online 27 DEC 2016

Published online 30 JAN 2017

## Winter respiratory C losses provide explanatory power for net ecosystem productivity

M. Haeni<sup>1,2</sup> , R. Zweifel<sup>1</sup>, W. Eugster<sup>2</sup> , A. Gessler<sup>1</sup> , S. Zielis<sup>2</sup> , C. Bernhofer<sup>3</sup> , A. Carrara<sup>4</sup> , T. Grünwald<sup>3</sup> , K. Havránková<sup>5</sup> , B. Heinesch<sup>6</sup>, M. Herbst<sup>7,8</sup>, A. Ibrom<sup>9</sup> , A. Knohl<sup>7</sup> , F. Lagergren<sup>10</sup> , B. E. Law<sup>11</sup> , M. Marek<sup>5</sup>, G. Matteucci<sup>12</sup> , J. H. McCaughey<sup>13</sup>, S. Minerbi<sup>14</sup>, L. Montagnani<sup>15</sup> , E. Moors<sup>16,17</sup> , J. Olejnik<sup>5,18</sup> , M. Pavelka<sup>5</sup> , K. Pilegaard<sup>9</sup> , G. Pita<sup>19</sup> , A. Rodrigues<sup>20</sup> , M. J. Sanz Sánchez<sup>21</sup> , M.-J. Schelhaas<sup>16</sup> , M. Urbaniak<sup>18</sup> , R. Valentini<sup>22</sup> , A. Varlagin<sup>23</sup> , T. Vesala<sup>24,25</sup> , C. Vincke<sup>6</sup> , J. Wu<sup>9,26</sup>, and N. Buchmann<sup>2</sup>

<sup>1</sup>Swiss Federal Research Institute WSL, Birmensdorf, Switzerland, <sup>2</sup>Institute of Agricultural Sciences, ETH Zürich, Zürich, Switzerland, <sup>3</sup>Institut für Hydrologie und Meteorologie, LS Meteorologie, TU Dresden, Tharandt, Germany, <sup>4</sup>Fundación CEAM, Valencia, Spain, <sup>5</sup>CzechGlobe-Global Change Research Institute CAS, Brno, Czech Republic, <sup>6</sup>Exchanges Ecosystem Atmosphere, University of Liege—Gembloux Agro-Bio Tech, TERRA, Gembloux, Belgium, <sup>7</sup>Bioclimatology, Georg-August-University of Göttingen, Göttingen, Germany, <sup>8</sup>Thünen Institute of Climate-Smart Agriculture, Braunschweig, Germany, <sup>9</sup>Department of Environmental Engineering, Technical University of Denmark, Kongens Lyngby, Denmark, <sup>10</sup>Department of Physical Geography and Ecosystem Science, Lund University, Lund, Sweden, <sup>11</sup>Forest Ecosystems and Society, Oregon State University, Corvallis, Oregon, USA, <sup>12</sup>Institute for Agricultural and Forestry Systems in the Mediterranean (ISAFOM), National Research Council of Italy, Ercolano (NA), Italy, <sup>13</sup>Department of Geography and Planning, Queen's University, Kingston, Ontario, Canada, <sup>14</sup>Ufficio Amministrazione Forestale, Bolzano, Italy, <sup>15</sup>Faculty of Science and Technology, Free University of Bolzano, Bolzano, Italy, <sup>16</sup>Climate Change and Adaptive Land and Water Management, Wageningen UR, Alterra, Wageningen, Netherlands, <sup>17</sup>Faculty of Earth and Life Sciences, VU University Amsterdam, Amsterdam, Netherlands, <sup>18</sup>Department of Meteorology, Poznań University of Life Sciences, Poznań, Poland, <sup>19</sup>Instituto Superior Técnico, Mechanical Engineering Department, University of Lisbon, Lisbon, Portugal, <sup>20</sup>Unidade Estratégica Investigação e Serviços de Sistemas Agrários e Florestais e Sanidade Vegetal, Instituto Nacional de Investigação Agrária e Veterinária, Oeiras, Portugal, <sup>21</sup>BC3 Basque Centre for Climate Change, Bilbao, Spain, <sup>22</sup>Department for Innovation in Biological, Agro-Food and Forest System, University of Tuscia, Viterbo, Italy, <sup>23</sup>A.N. Severtsov Institute of Ecology and Evolution, Russian Academy of Sciences, Moscow, Russia, <sup>24</sup>Department of Physics, University of Helsinki, Helsinki, Finland, <sup>25</sup>Department of Forest Sciences, University of Helsinki, Helsinki, Finland, <sup>26</sup>Zhejiang Provincial Key Laboratory of Forest Intelligent Monitoring and Information Technology, Zhejiang A&F University, Hangzhou, China

**Abstract** Accurate predictions of net ecosystem productivity ( $NEP_c$ ) of forest ecosystems are essential for climate change decisions and requirements in the context of national forest growth and greenhouse gas inventories. However, drivers and underlying mechanisms determining  $NEP_c$  (e.g., climate and nutrients) are not entirely understood yet, particularly when considering the influence of past periods. Here we explored the explanatory power of the compensation day (cDOY)—defined as the day of year when winter net carbon losses are compensated by spring assimilation—for  $NEP_c$  in 26 forests in Europe, North America, and Australia, using different  $NEP_c$  integration methods. We found cDOY to be a particularly powerful predictor for  $NEP_c$  of temperate evergreen needleleaf forests ( $R^2 = 0.58$ ) and deciduous broadleaf forests ( $R^2 = 0.68$ ). In general, the latest cDOY correlated with the lowest  $NEP_c$ . The explanatory power of cDOY depended on the integration method for  $NEP_c$ , forest type, and whether the site had a distinct winter net respiratory carbon loss or not. The integration methods starting in autumn led to better predictions of  $NEP_c$  from cDOY than the classical calendar method starting 1 January. Limited explanatory power of cDOY for  $NEP_c$  was found for warmer sites with no distinct winter respiratory loss period. Our findings highlight the importance of the influence of winter processes and the delayed responses of previous seasons' climatic conditions on current year's  $NEP_c$ . Such carry-over effects may contain information from climatic conditions, carbon storage levels, and hydraulic traits of several years back in time.

### 1. Introduction

Accurate predictions of carbon dioxide ( $CO_2$ ) exchange by forest ecosystems are essential for understanding, e.g., the role of the forest mitigation in the context of the National Determined Contribution under the Paris Agreement, as well as for the required estimates of annual carbon (C) budgets to be provided at national or

international level. Research in the past decades focused on improving these predictions on both annual and longer (decadal) timescales, e.g., in relation to extreme events [e.g., Baldocchi and Wilson, 2001; Ciais et al., 2005; Richardson et al., 2009; Rodrigues et al., 2011; Wolf et al., 2013; Wu et al., 2013] and in relation to the length of the growing seasons or the number of carbon uptake days [e.g., Churkina et al., 2005]. Our study builds on the current understanding that some critical periods within the current or the past year (e.g., winter frost and spring drought) may explain the interannual variability of C uptake of forests better than average conditions over the current year only [Le Maire et al., 2010]. The effects of climatic conditions from previous seasonal periods on current year's annual net ecosystem productivity ( $NEP_c$ ) are called carry-over effects and were quantified, e.g., by Shao et al. [2016], Thomas et al. [2009], and Zielis et al. [2014]. Such carry-over effects support the influence of specific periods in the past on current year's  $NEP_c$ , and their influence have been demonstrated a long time ago by tree ring analyses, e.g., for Danish forests [Holmsgaard, 1955]. Here we use positive  $NEP$  defined as net C uptake, while negative  $NEP$  is a net C release to the atmosphere ( $NEE$  is defined with the opposite sign in Aubinet et al. [2012]). Further,  $NEP_c$  is defined as the cumulative sum of  $NEP$  fluxes throughout the annual cycle—not necessarily a calendar year—yielding net C flux between the atmosphere and the forest. To account for the temporal integration of the average  $NEP_c$  over an annual cycle, values are expressed in  $g\ C\ m^{-2}\ yr^{-1}$ , whereas half-hourly  $NEP$  measurements are given in  $g\ C\ m^{-2}\ s^{-1}$  (as calculated from  $\mu\ mol\ m^{-2}\ s^{-1}$ ).

### 1.1. The Concept of cDOY

Following the concept of previous year's weather conditions influencing current year  $NEP_c$ , we explored the information content of cDOY, defined as the day of year when the net carbon losses accumulated during the wintertime are compensated by net assimilation in spring. The timing of cDOY is assumed to change with climatic conditions of previous periods (of unknown length) and may have a direct impact on the current year  $NEP_c$  [Zielis et al., 2014]. Similar approaches were described in literature, e.g., the "zero-crossing time," wherein net ecosystem exchange is used to define the time when the forest ecosystem turns from a C source in winter into a C sink in spring [Gonsamo et al., 2012a; Gonsamo et al., 2012b]. Another approach quantifies the so-called "start of the carbon uptake period" which is determined by a sharp increase in gross primary production (GPP) [Delpierre et al., 2009]. However, these approaches rely on instant net ecosystem exchange rates only and do not accumulate carbon loss over an entire wintertime, as it is the case of in the cDOY approach.

### 1.2. Integration Methods for $NEP_c$

Traditionally,  $NEP_c$  is integrated annually over a time period of the Gregorian calendar year (classical integration as shown in Figure 1). This is more a practical choice, but it neither reflects any particular connection to underlying carbon cycle processes nor does it take into account potential carry-over effects on  $NEP_c$ . As an example, trees prepare their buds in autumn and thus the predisposition for growth (and thus  $NEP_c$ ) during the following season is determined in autumn already. Thus, it is important to consider the start and end of the accumulation period of  $NEP_c$ . In line with these thoughts, Urbanski et al. [2007] introduced a method integrating  $NEP_c$  at Harvard Forest from 28 October to 27 October of the following year (Urbanski integration in Figure 1), trying to come closer to a more reasonable biological time reference of the annual  $NEP$  cycle. This integration period is similar to the hydrological year as starting on 1 November in the Northern Hemisphere. Thomas et al. [2009] found that interannual and seasonal variations in carbon and water processes were best explained when seasonality was defined functionally within hydrological years.

More recently, a dynamic integration approach was introduced by Zweifel et al. [2010] in order to relate continuous stem diameter fluctuations to  $NEP_c$ . The frequently occurring stem shrinkages induced by winter frost [Zweifel and Hasler, 2000] made the classical integration approach from 1 January to 31 December inapplicable for an unbiased analysis of annual stem growth increments (bark and wood) in relation to  $NEP_c$ . An integration over a variable period was therefore proposed (Figure 1), starting with the day when  $NEP_c$  of the previous calendar year reached its maximum and ending with the day in the current year when maximum  $NEP_c$  was achieved (dynamic integration in Figure 1). Thus, the dynamic year corresponds more closely to the actual biological cycle, which does not exactly count 365.25 days per year. This dynamic integration method is appropriate to time series of stem increments and  $NEP_c$  data from eddy covariance flux measurements. It was concluded that the application of this approach reduces distortion effects on annual sums, due to apparent interannual variations in carbon losses and stem shrinkages during wintertime [Zweifel et al.,

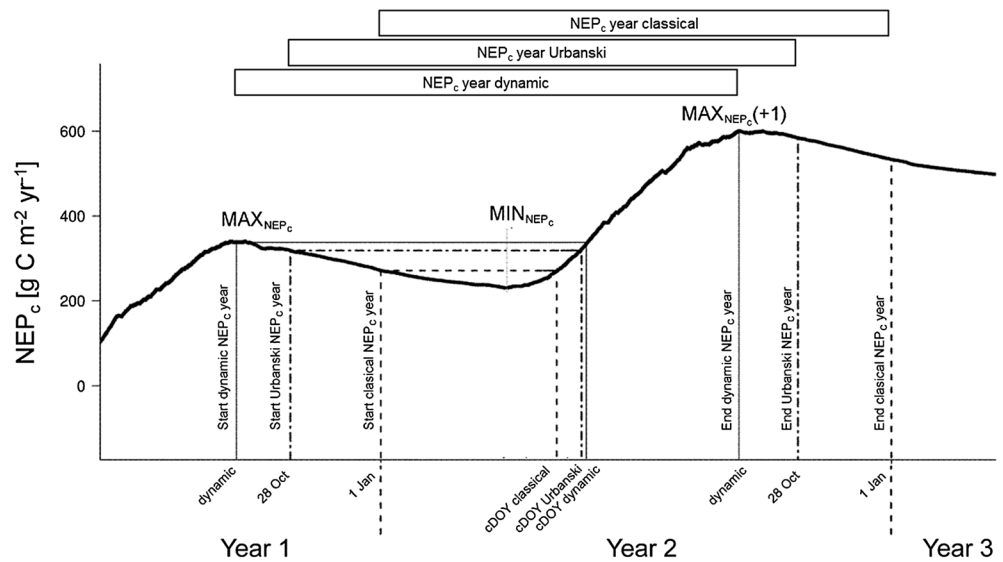


**Figure 1.** Three different methods of integrating net ecosystem productivity ( $NEP_c$ ) over time (real data shown: Hyytiälä, years 2010 to 2012): Classical integration runs from 1 January to 31 December of each calendar year, “current” is year 2; Urbanski integration from 28 October of the previous year to the end of 27 October of the current year; Dynamic integration runs dynamically for every site and for every year from the day of the previous year’s cumulated  $NEP_c$  maximum ( $MAX_{NEP_c}$ ) to the current year’s cumulated  $NEP_c$  maximum ( $MAX_{NEP_c} (+1)$ ). Net carbon losses occur between  $MAX_{NEP_c}$  and the minimum of  $NEP_c$  of the current year ( $MIN_{NEP_c}$ ). The day of compensation (cDOY) is defined as the day of the year when  $MAX_{NEP_c}$  (of the previous year) is crossed by  $NEP_c$  in the current year. Accordingly, cDOY depends on the integration method. For the Southern Hemisphere, i.e., for the Australian site AU-Tum, the same cuts were made, one half year later. The corresponding year started on 1 July and ended on 30 June.

2010], i.e., shifts in uptake and loss periods that arbitrarily affect the sums calculated over a fixed calendar period. We use the terms “year” and “annual” in combination with all three integration methods, for the sake of readability, being aware that the terms usually are implicitly used for periods of Gregorian calendar years from 1 January to 31 December.

The way of splitting time series into annual integration periods also changes the potential contribution of winter carbon losses for the total annual C uptake and the cDOY timing in the following year (Figure 1). Indeed, the classical integration period splits the net carbon loss of a winter period in two parts, assigning them to two different  $NEP_c$  years, while the dynamic (and Urbanski) integration method assigns net carbon loss for all the winter period entirely to the  $NEP_c$  of the biological year that will last until the onset of the next winter period. Accordingly, cDOY changes with the respective integration method (Figure 1) and might have a different explanatory power for  $NEP_c$ .

In this study, we used in total 26 eddy covariance forest sites with 25 sites throughout Europe and North America (Figure 2), and additionally one site from Australia, thus covering a wide range of climatic conditions (Table 1) to investigate the meaning of cDOY for  $NEP_c$  and its underlying drivers. We used the cDOY timing as the key measure associated with the net carbon loss period and related it to climatic conditions and  $NEP_c$ . We addressed the following specific objectives: (1) application of three different  $NEP_c$  integration methods (classical, Urbanski, and dynamic) in order to calculate and compare the respective cDOYs, (2) identification of climatic and biological drivers for cDOY across sites and across different years, (3) evaluation of different cDOY as a predictor for its associated  $NEP_c$ , and (4) the weight of winter net respiratory losses on current year’s  $NEP_c$ .

## 2. Materials and Methods

### 2.1. Study Sites

The study is based on carbon dioxide ( $CO_2$ ) flux data from 347 site years from 26 eddy covariance (EC) forest sites (managed forest not affected by major disturbances like fire or wind throw) within Europe, North America, and Australia (Table 1 and Figure 2). The selected sites fulfilled the following criteria: (1) at least

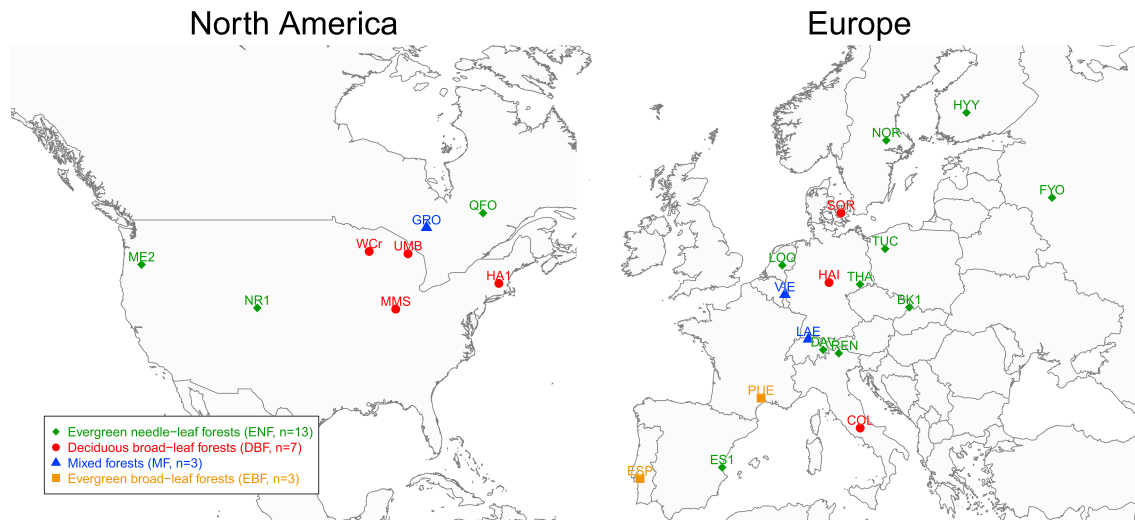


**Figure 2.** Spatial distribution of 25 sites across North America and Europe and one Australian site (not shown). Site abbreviations are listed in Table 1. ENF = evergreen needleleaf forests, DBF = deciduous broadleaf forests, MF = mixed forests, and EBF = evergreen broadleaf forests.

4 years of continuous EC data, (2) availability of Level 4 (L4) data quality according to the European Fluxes Database [European Fluxes Database Cluster, 2014] or available from the FluxNet2015 data set (<http://fluxnet.fluxdata.org/data/fluxnet2015-dataset/>), and (3) available meteorological and forest characteristics data. The forest vegetation at the sites was classified as deciduous broadleaf forests (DBF,  $n = 7$ ), mixed forest (MF,  $n = 3$ ), evergreen needleleaf forests (ENF,  $n = 13$ ), and evergreen broadleaved forest (EBF,  $n = 3$ ).

## 2.2. CO<sub>2</sub> Flux Measurements

Half-hourly or hourly CO<sub>2</sub> flux data (net ecosystem exchange rates summed up to net ecosystem productivity, NEP), derived from both open- and closed-path gas analyzers, were downloaded from the FluxNet2015 data set (<http://fluxnet.fluxdata.org/data/fluxnet2015-dataset/>) or in L4 quality from the European Fluxes Database (<http://www.europe-fluxdata.eu/home>). These data were already filtered and gap filled (Table 1). For three sites (CH-DAV, CH-LAE, and PL-TUC, all open-path gas analyzers) our own site-specific processing was conducted: data were filtered for unfavorable atmospheric conditions such as snow, heavy rain, and/or dust which increased window dirtiness of the infrared gas analyzer > 70%. For these three individual sites, the threshold for insufficient nocturnal turbulent mixing of the atmosphere (determined via the friction velocity  $u_*$  for mechanical turbulence) was determined with the online EC gap-filling and flux partitioning tool (Markus Reichstein and Olaf Menzer, <http://www.bgc-jena.mpg.de/~MDIwork/eddyproc/>) [Reichstein *et al.*, 2013; Reichstein *et al.*, 2005] and was found to be  $0.2 \text{ m s}^{-1}$ .

## 2.3. CO<sub>2</sub> Flux Integration

Annual NEP<sub>c</sub> was integrated with three different methods (Figure 1): classical method: NEP<sub>c</sub> is integrated from January 1 to December 31; Urbanski method: NEP<sub>c</sub> is integrated from 28 October to 27 October 1 year later [Urbanski *et al.*, 2007]; and dynamic method: integration of NEP<sub>c</sub> from the DOY with the maximum seasonal peak of the previous year (typically in fall; MAX<sub>NEP<sub>c</sub></sub>) to the DOY with MAX<sub>NEP<sub>c</sub></sub> of the current year (Figure 1). The dynamic integration method led to “annual cycles” ranging from 7 to 16 months depending on year and site; the overall average was 364 days (supporting information Figure S1). For the Southern Hemisphere site AU-Tum, the year has been shifted half a year forward, i.e., the classical year started with 1 July and the dynamic “integration period” started with the maximum peak (MAX<sub>NEP<sub>c</sub></sub>) before 1 July. The Urbanski integration method was not applied for this site.

## 2.4. Statistical Analyses

Statistical analyses were performed using the statistical software R, version 3.3.1 [R Development Core Team, 2013]. All multiple regression models were based on linear relationships. Adjusted  $R^2$  (adj $R^2$ ) was used for the quantification of goodness of fit. Analyzed potential drivers for cDOY are listed in Table 1. Their respective impacts on cDOY were analyzed with multiple regression models based on the inclusion of explaining

**Table 1.** Selected Characteristics of the Study Sites (See Also Figure 2)<sup>a</sup>

Code	Name	Forest Type	Lat.	Long.	Year Range	MAP	MAT	Altitude	Age	Height	LAI	N	Data Access	Data in This Table From
AU-TUM	Tumbarumba	EBF	-35.66	148.15	2002–2013	1924	9.6	1249	100	40	2.5	--	FluxNet2015	Beringer et al. [2016]; FluxNet2015 meta*; pc*
BE-VIE	Vielsalm	MF	50.31	6	1997–2014	1062	7.8	493	95	35	4.6	10.2	FluxNet2015	Flechar et al. [2011]; FluxNet2015 meta; pc
CA-GRO	Ontario, Groundhog River, Boreal Mixed wood Forest	MF	48.22	-82.16	2004–2013	831	1.3	340	84	32	--	--	FluxNet2015	McCaughy et al. [2006], Gökkyaya et al. [2014], and Gökkyaya et al. [2015]; FluxNet2015 meta; pc
CA-QFO	Quebec, Eastern Boreal, Mature Black Spruce	ENF	49.69	-74.34	2004–2010	962	-0.4	382	105	13.8	3.7	--	FluxNet2015	Coursolle et al. [2012]; FluxNet2015 meta; pc
CH-DAV	Davos	ENF	46.81	9.86	1997–2011	1046	3.5	1662	240	25	3.9	1.5	own site	own site; FluxNet2015 meta
CH-LAE	Lägeren	MF	47.48	8.37	2004–2011	1211	8.7	682	140	31	3.6	14.3	own site	Flechar et al. [2011]; FluxNet2015 meta
CZ-BK1	Bily Kriz	ENF	49.5	18.54	2001–2010	1316	6.7	875	30	10	7.5	10.5	download, L4	Flechar et al. [2011]; pc
DE-HAI	Hainich	DBF	51.08	10.45	2000–2012	720	8.3	430	125	33	6	12.6	FluxNet2015	Knohl et al. [2003], Mund et al. [2010], Flechar et al. [2011], and Herbst et al. [2015]; FluxNet2015 meta; pc
DE-THA	Tharandt	ENF	50.96	13.57	1997–2014	820	7.7	385	125	26.5	7.6	12.5	FluxNet2015	Grünwald and Bernhofer [2007] and Flechar et al. [2011]; FluxNet2015 meta; pc
DK-SOR	Soroe	DBF	55.49	11.65	1997–2014	660	8.2	40	100	35	4.8	14.6	FluxNet2015	FluxNet2015 meta; pc
ES-ES1	El Saler	ENF	39.35	-0.32	2000–2007	551	17.9	1	100	10	3.5	16.9	download, L4	FluxNet2015 meta; pc
FI-HYY	Hyytiälä	ENF	61.85	24.3	1997–2014	709	3.8	181	40	14	2.5	3.5	download, L4	Flechar et al. [2011]; FluxNet2015 meta; pc
FR-PUE	Puechabon	EBF	43.74	3.6	2000–2014	883	13.5	270	73	5.5	2.9	--	FluxNet2015	Flechar et al. [2011]; FluxNet2015 meta; pc
IT-COL	Collelongo	DBF	41.85	13.59	1997–2011	1180	6.3	1645	105	25	5	5.3	download, L4	Scartazza et al. [2016] and Flechar et al. [2011]; FluxNet2015 meta; pc
IT-LAV	Lavarone	ENF	45.96	11.28	2003–2014	1291	7.8	1353	100	28	8.1	15.4	FluxNet2015	FluxNet2015 meta; pc
IT-REN	Renon	ENF	46.59	11.43	1999–2013	809	4.7	1730	200	31	5.1	4.8	FluxNet2015	Flechar et al. [2011]; FluxNet2015 meta; pc
NL-LOO	Loobos	ENF	52.17	5.74	1997–2013	966	10	25	90	18	1.9	32.4	FluxNet2015	Flechar et al. [2011]; FluxNet2015 meta; pc
PL-TUC	Tuczno	ENF	53.21	16.1	2008–2011	625	7.8	105	54	20	1.1	8.5	STSM, direct	FluxNet2015 meta; pc
PT-ESP	Espirra	EBF	38.64	-8.6	2002–2008	665	15.4	85	12	20	3.1	7.2	download, L4	FluxNet2015 meta; pc
RU-FYO	Fyodorovskoye	ENF	56.46	32.92	1998–2014	711	3.9	265	196	25.7	3.5	8.3	FluxNet2015	Rodrigues et al. [2011], and Flechar et al. [2011]; pc
SE-NOR	Norunda	ENF	60.09	16.22	1996–2011	527	5.5	45	100	25	5	3.4	STSM, direct	Flechar et al. [2011]; FluxNet2015 meta; pc
US-HA1	Harvard Forest EMS Tower (HFR1)	DBF	42.54	-72.15	1992–2012	1071	6.6	340	80	18	3.7	6.4	FluxNet2015	Lagergren et al. [2008] and Flechar et al. [2011]; pc
US-ME2	Metolius-intermediate aged ponderosa pine	ENF	44.45	-121.55	2002–2014	523	6.3	1253	90	14	3.2	1	FluxNet2015	Munger et al. [1996] and Munger et al. [1998]; FluxNet2015 meta; pc



**Table 1.** (continued)

Code	Name	Forest Type	Lat.	Long.	Year Range	MAP	MAT	Altitude	Age	Height	LAI	N	Data Access	Data in This Table From
US-MMS	Morgan Monroe State Forest	DBF	39.92	-86.41	1999–2014	1032	10.9	275	90	27	4.7	6	FluxNet2015	Schwarz <i>et al.</i> [2004] and Thomas <i>et al.</i> [2009]; FluxNet2015 meta; pc
US-NR1	Niwot Ridge Forest (LTER NWT1)	ENF	40.03	-105.55	1999–2014	800	1.5	3050	115	13	4	6	FluxNet2015	Schmid <i>et al.</i> [2000], Dragoni <i>et al.</i> [2011], Brzostek <i>et al.</i> [2014], and Roman <i>et al.</i> [2015]; FluxNet2015 meta; pc
US-UMB	Univ. of Mich. Biological Station	DBF	45.56	-84.71	2000–2014	803	5.38	234	93	22	3.5	7.5	FluxNet2015	Sievering <i>et al.</i> [2001]; FluxNet2015 meta; pc
US-WCR	Willow Creek	DBF	45.8	-90.08	1999–2014	787	4.02	520	70	24.2	5.36	--	FluxNet2015	Gough <i>et al.</i> [2008], Nave <i>et al.</i> [2009], and Gough <i>et al.</i> [2013]; FluxNet2015 meta; pc

<sup>a</sup>Site names are abbreviated with the FLUXNET codes. Forest types are abbreviated as DBF = deciduous broadleaf forests, ENF = evergreen needleleaf forests, MF = mixed forests, and EBF = evergreen broadleaf forests. Further terms in the header have the following meaning: Lat., Latitude (degrees, WGS84) and Long. = Longitude (degrees, WGS84) of the site. Year Range = data of the indicated years used in this study. MAP = mean annual sum of precipitation (mm). MAT = mean annual air temperature (°C) at the top of the eddy towers; Altitude = meter above sea level (masl); Age = average age of the mature trees in the stand (years); Height = maximum tree height (m); LAI = leaf area index (m<sup>2</sup> m<sup>-2</sup>); N = mean annual nitrogen deposition (kg ha<sup>-1</sup> yr<sup>-1</sup>), most data and where stated from Flechard *et al.* [2011]; Data access: NEP<sub>c</sub> data were obtained from European Database Cluster in Level 4 quality, from the FluxNet2015 data set or from the respective PIs incl. own sites (see section 2). Site characteristics were obtained from <https://fluxnet.ornl.gov>, from the \*FluxNet2015 Metadata excel sheet, from <http://www.bgc-jena.mpg.de/public/carboeur/sites/SITE.html>, or from \*personal communication (pc). Not available data are indicated with “-”. References in Table 1 are as follows: Beringer *et al.* [2016], Brzostek *et al.* [2014], Cook *et al.* [2004], Coursolle *et al.* [2012], Dragoni *et al.* [2011], Flechard *et al.* [2014], Gökkyaya *et al.* [2014], Gough *et al.* [2008], Gough *et al.* [2015], Herbst *et al.* [2015], Keith *et al.* [2012], Knohl *et al.* [2003], Lagergren *et al.* [2008], McCaughy *et al.* [2006], Mund *et al.* [2010], Munger *et al.* [1998], Munger *et al.* [1996], Nave *et al.* [1996], Pilegaard *et al.* [2011], Pita *et al.* [2013], Rodrigues *et al.* [2011], Roman *et al.* [2015], Scartazza *et al.* [2016], Schmid *et al.* [2000], Schwarz *et al.* [2004], Sievering *et al.* [2001], and Thomas *et al.* [2009].

variables in a stepwise way. The so-called standardized regression coefficients ( $\beta$  coefficients) were used to determine the relative importance of variables (var) within the models, ranging between  $-1$  as the highest negative and  $+1$  as the highest positive correlative importance [Quinn and Keough, 2002]. A  $\beta$  coefficient close to zero indicates that the variable does not add to the quality of the model.

### 3. Results

#### 3.1. Compensation of Net Carbon Loss After Wintertime

The day of year when respiratory carbon losses from the previous winter were compensated (cDOY) differed strongly across sites (Table 2 and Figure 3). cDOY varied from 3 January (AU-TUM/3 July) to 25 July (CA-QFO), with a mean of 3 May (obtained by averaging all three integration methods, Figure 3). Some sites showed no or irregular cDOY timings, meaning that they observed no distinct respiratory carbon loss period every year (Table 2). Evergreen forests ( $3 \times$  EBF,  $13 \times$  ENF) in general had an earlier cDOY (18 April) than deciduous forests ( $7 \times$  DBF, June 28). Only nine out of the 26 sites compensated on average their net carbon losses in the climatologically defined spring calendar months (Mar–May) (Table 2). Six sites compensated before spring, while eleven compensated after May. The yearly standard deviation of cDOY for individual sites ranged from 6 days (DE-HAI, AU-TUM) to more than 50 days (PT-ESP) (Table 2).

Further, cDOY strongly depended on the integration method. In general, the classical integration method led to a cDOY almost 3 weeks earlier than those obtained with the dynamic method (classical: 16 April; dynamic: 10 May). The average cDOY obtained from the Urbanski integration method (5 May) was almost the same as that from the dynamic method (data now shown). Much less affected were the mean differences (Urbanski versus classical:  $-54 \text{ g C m}^{-2} \text{ yr}^{-1}$  and dynamic versus classical:  $-91 \text{ g C m}^{-2} \text{ yr}^{-1}$ ) and the standard deviations (Urbanski versus classical:  $-7 \text{ g C m}^{-2} \text{ yr}^{-1}$  and dynamic versus classical:  $-10 \text{ g C m}^{-2} \text{ yr}^{-1}$ ) of  $\text{NEP}_c$  between the different integration methods (see also supporting information figures for each site).

#### 3.2. Drivers of cDOY

Average cDOY was substantially correlated with mean annual air temperature ( $R^2$  between 0.4 and 0.45). The relationship was largely independent of the integration method used (Table 3), and the later cDOYs corresponded to the cooler sites (Figure 3a). Other site characteristics considered (latitude, longitude, altitude, tree age, nitrogen deposition, tree height, and mean annual precipitation) showed weak (or no) linear relationship to cDOY and did not improve the stepwise multiple linear regression models to explain cDOY (Table 3).

The meaning of mean annual site temperature (MAT) for cDOY was markedly increased when the pooled data over all sites were grouped into four forest types (Figure 3a): evergreen needleleaf forest (ENF, all included), evergreen broadleaf forest (EBF), and mixed forest (MF) showed  $R^2$  between 0.64 and 0.99. No significant correlation was found between MAT and cDOY for the deciduous broadleaf forests (DBF;  $R^2 = 0.07$ ,  $p > 0.05$ ).

In Figure 3b, those sites without a distinct winter respiratory loss period, and thus with no consistent cDOY timing (Table 2) were removed (all EBF and more than 50% of the ENF sites). All of these sites are evergreen, with a majority having MAT over  $8\text{--}10^\circ\text{C}$ ; hence, in winter, these sites likely photosynthesize. The remaining six ENF sites (CA-QFO, CH-DAV, FI-HYY, RU-FYO, SE-NOR, and US-NR1), with a distinct winter respiratory loss and a latter cDOY, increase to an  $\text{adj}R^2$  of 0.90 for the linear relationship between MAT and cDOY (Figure 3b).

#### 3.3. Relationship Between cDOY and $\text{NEP}_c$

The 26 sites analyzed in this study included C sink and C source sites (Table 2). The largest net annual respiratory loss was at RU-FYO with a consistent average C output of  $137 \text{ g C m}^{-2} \text{ yr}^{-1}$ . The largest net C uptake was at AU-TUM with  $1007 \text{ g C m}^{-2} \text{ yr}^{-1}$ .

Stepwise multivariate analysis showed that cDOY, among the site characteristic variables available, explained most of  $\text{NEP}_c$  for all integration methods (Table 4). Sites with distinct winter respiratory loss, explained significantly more of  $\text{NEP}_c$  than all other sites. cDOY obtained from the two integration approaches that initiated the  $\text{NEP}_c$  year in autumn (Urbanski and dynamic) explained  $\text{NEP}_c$  significantly better ( $\text{adj}R^2 = 0.35$  and  $0.47$ ) than cDOY from the classical integration approach ( $\text{adj}R^2 = 0.23$ ). When the ENF (Table 4d) and DBF (Table 4e) sites were analyzed separately (using the dynamic integration), the  $R^2$  of the linear regressions was further improved ( $R^2$  of 0.58 and 0.68, respectively).

**Table 2.** NEP<sub>c</sub> Averages, cDOY Averages, and Relationships Between Compensation Days (cDOY = Day of Year When Winter Respiratory Losses Were Compensated) and Integrated Net Ecosystem Productivity (NEP<sub>c</sub>) for Each Site and Integration Method (Classical, Urbanski, and Dynamic)<sup>a</sup>

Site	Mean NEP <sub>c</sub>	n cDOY Cla.	n cDOY Urb.	n cDOY Dyn.	cDOY	R <sup>2</sup> Cla.	p Cla.	R <sup>2</sup> Urb.	p Urb.	R <sup>2</sup> Dyn.	p Dyn.	Average SD NEP <sub>c</sub>	% Winter Resp. Loss	Classification
AU-TUM	1006.7 ± 273.4	12	--	12	Jul 03 ± 6	0.05	0.48	--	--	0.05	0.51	159.9	5.4%	without
BE-VIE	461.9 ± 155.6	18	18	18	Apr 29 ± 28	0.62	0.00	0.73	0.00	0.74	0.00	173.3	-19.8%	with
CA-GRO	120.6 ± 47.3	10	10	10	Jun 27 ± 15	0.40	0.05	0.52	0.02	0.70	0.00	52.8	-143.6%	with
CA-QFO	2.8 ± 14.5	7	7	3	Jul 23 ± 23	0.08	0.54	0.24	0.26	0.01	0.93	14.7	-420.3%	with
CH-DAV	134.1 ± 70.8	15	15	15	Mai 28 ± 34	0.74	0.00	0.88	0.00	0.87	0.00	74.0	-80.8%	with
CH-LAE	579.7 ± 124.5	8	7	8	Mai 10 ± 14	0.76	0.00	0.72	0.02	0.68	0.01	122.2	-16.1%	with
CZ-BK1	798.9 ± 132.8	10	10	10	Apr 04 ± 8	0.07	0.45	0.00	0.94	0.00	0.95	128.9	-6.6%	without
DE-HAI	579.2 ± 73.2	13	13	13	Jun 21 ± 6	0.12	0.25	0.12	0.25	0.06	0.42	68.0	-51.4%	with
DE-THA	617.9 ± 81.1	18	18	18	Apr 01 ± 18	0.16	0.10	0.18	0.08	0.20	0.07	81.7	-7.5%	without
DK-SOR	176 ± 139.4	18	18	16	Jun 26 ± 18	0.66	0.00	0.84	0.00	0.82	0.00	151.7	-88.6%	with
ES-ES1	415.5 ± 154.9	8	6	8	Jan 27 ± 27	0.06	0.57	0.01	0.85	0.47	0.06	164.9	-3.6%	without
FI-HYY	244.9 ± 50.5	16	16	16	Mai 26 ± 10	0.19	0.10	0.53	0.00	0.59	0.00	53.3	-41.6%	with
FR-PUE	230.5 ± 89.2	14	12	14	Feb 01 ± 22	0.01	0.72	0.19	0.16	0.06	0.41	88.1	-8.6%	without
IT-COL	622 ± 179	13	13	13	Jun 09 ± 10	0.45	0.01	0.53	0.00	0.53	0.00	179.8	-28.2%	with
IT-REN	248 ± 96.7	12	12	12	Mai 10 ± 28	0.11	0.29	0.04	0.52	0.03	0.61	85.9	-7.4%	without
NL-LOO	427.5 ± 144.6	17	16	17	Mtz 22 ± 41	0.52	0.00	0.60	0.00	0.70	0.00	160.7	-9.7%	without
PL-TUC	667.5 ± 76.1	4	1	4	Jan 28 ± 30	0.53	0.28	0.00	--	0.70	0.16	82.9	0.1%	without
PT-ESP	459.7 ± 356.6	6	2	6	Feb 02 ± 50	0.48	0.13	1.00	--	0.51	0.11	363.0	-6.5%	without
RU-FYO	-136.7 ± 128.2	11	8	2	Jun 13 ± 26	0.33	0.07	0.19	0.29	1.00	--	145.4	104.7%	with
SE-NOR	52.8 ± 33.8	15	15	12	Apr 15 ± 31	0.67	0.00	0.86	0.00	0.51	0.01	37.1	-52.0%	with
US-HAI	211.2 ± 188	21	19	19	Jul 24 ± 22	0.54	0.00	0.75	0.00	0.78	0.00	102.5	-401.0%	with
US-ME2	588 ± 291.2	13	5	13	Feb 08 ± 40	0.59	0.00	0.76	0.05	0.67	0.00	316.6	-0.9%	without
US-MMS	428.6 ± 75.8	16	16	16	Jun 20 ± 9	0.15	0.14	0.19	0.09	0.24	0.05	39.3	-60.9%	with
US-NR1	170.7 ± 30.1	16	16	16	Jun 02 ± 9	0.01	0.71	0.09	0.25	0.12	0.19	31.8	-48.3%	with
US-UMB	268.9 ± 65.8	15	15	15	Jul 04 ± 10	0.19	0.10	0.27	0.05	0.34	0.02	31.4	-80.5%	with
US-WCR	271.9 ± 153.6	12	12	11	Jun 29 ± 41	0.35	0.04	0.55	0.01	0.67	0.00	164.6	-89.7%	with

<sup>a</sup>Mean NEP<sub>c</sub> = mean annual net ecosystem productivity and standard deviation (gm<sup>-2</sup> yr<sup>-1</sup>), averaged over all three integration methods (classical, Urbanski, and dynamic); n cDOY = show many cDOYs could be calculated for each of the integration methods; Mean cDOY = mean NEP<sub>c</sub> compensation day of the years investigated including standard deviations. Average SD NEP = standard deviation of NEP<sub>c</sub> averaged over all three integration methods; % winter respiratory loss = average percentage of winter respiratory loss from average NEP<sub>c</sub> classification into whether the site is a site with or without distinct winter respiratory loss (threshold is <10%).



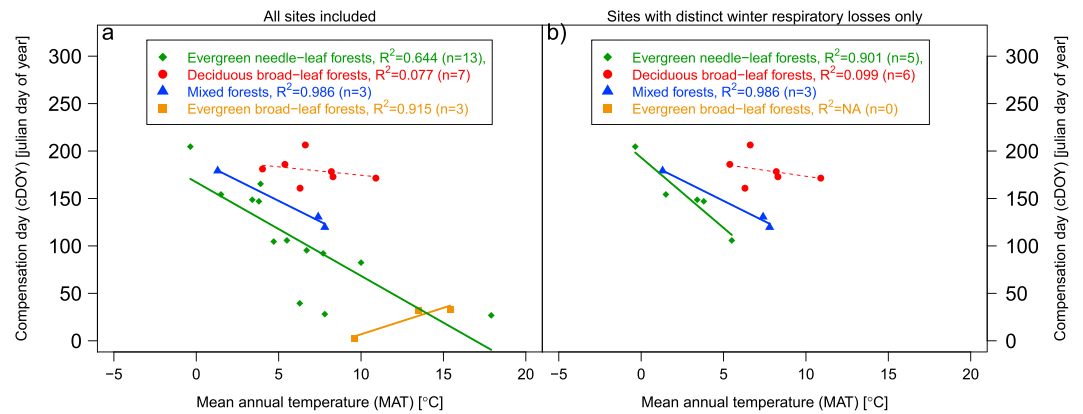


**Figure 3.** Relationship between cDOY (integrated dynamically) and mean annual temperature (MAT) grouped for the four forest types. (a) All sites included ( $n = 26$ ) and (b) sites with distinct winter respiratory losses only, i.e., where winter net respiration loss accounts for more than 10% of the annual net ecosystem productivity and  $n$  was  $> 2$  for all integration methods.

**Table 3.** Stepwise Multiple Linear Regression Models to Determine the Drivers of the Day of Compensation cDOY for the Classical, Urbanski, and Dynamic Integration Method<sup>a</sup>

Drivers of cDOY	$R^2$ Alone	1 Var	2 Vars	3 Vars	4 Vars	5 Vars	6 Vars	7 Vars
<i>Classical Integration Method</i>								
MAT	0.4***	-0.63	-0.58	-0.57	-0.58	-0.53	-0.55	-0.48
LAI	0.11	--	0.25	0.25	0.23	0.13	0.14	0.03
Age	0.06	--	--	0.03	-0.02	-0.06	-0.03	0.06
Height	0.05	--	--	--	0.1	0.29	0.27	0.23
N	0.03	--	--	--	--	0.08	0.07	-0.05
Altitude	0.01	--	--	--	--	--	-0.07	-0.19
MAP	0	--	--	--	--	--	--	0.37
Total adj $R^2$	--	0.4***	0.39***	0.36**	0.34**	0.17*	0.12*	0.21*
<i>Urbanski Integration Method</i>								
MAT	0.45***	-0.67	-0.61	-0.58	-0.59	-0.61	-0.43	-0.5
Height	0.17*	--	0.29	0.29	0.31	0.34	0.35	0.27
MAP	0.1	--	--	0.21	0.21	0.21	0.28	0.33
Age	0.07	--	--	--	-0.06	-0.09	-0.04	0.06
LAI	0.06	--	--	--	--	-0.01	-0.03	-0.01
N	0.05	--	--	--	--	--	-0.06	-0.12
Altitude	0.01	--	--	--	--	--	--	-0.24
Total adj $R^2$	--	0.45***	0.48***	0.51***	0.49***	0.45***	0.23*	0.21*
<i>Dynamic Integration Method</i>								
MAT	0.4***	-0.63	-0.57	-0.57	-0.57	-0.5	-0.43	-0.52
LAI	0.1	--	0.23	0.23	0.22	0.1	0.01	0.04
Age	0.06	--	--	0.03	0	-0.06	-0.03	0.1
Height	0.03	--	--	--	0.06	0.36	0.36	0.24
N	0.03	--	--	--	--	0.04	-0.02	-0.09
MAP	0.01	--	--	--	--	--	0.23	0.3
Altitude	0	--	--	--	--	--	--	-0.33
Total adj $R^2$	--	0.4***	0.37**	0.34**	0.31**	0.2*	0.2*	0.22*

<sup>a</sup>The variables were included one by one in the models (MAT = mean annual air temperature at the top of the eddy towers; LAI = leaf area index; Age = average age of the mature trees in the stand; Height = maximum tree height; N = mean annual nitrogen deposition; MAP = mean annual sum of precipitation). The  $\beta$  coefficients (var) indicate the relative importance of the variable, ranging from  $-1$  (highest importance, negative correlation) to  $+1$  (highest importance, positive correlation). The first column gives the  $R^2$  for individual site characteristics (see Table 1).

\* $p < 0.05$ ,  
 \*\* $p < 0.01$ ,  
 \*\*\* $p < 0.001$ .

**Table 4.** Stepwise Multiple Linear Regression Models to Determine the Drivers of Net Ecosystem Productivity  $NEP_c$  for the Classical (All Sites), Urbanski (All Sites), and Dynamic Integration Method (All Sites)<sup>a</sup>

Drivers of $NEP_c$	$R^2$ Alone	1 Var	2 Vars	3 Vars	4 Vars	5 Vars	6 Vars	7 Vars	8 Vars
<i>Classical Integration Method (All Sites)<sup>b</sup></i>									
cDOY	0.23*	-0.48	-0.48	-0.39	-0.44	-0.38	-0.36	-0.59	-0.6
MAP	0.22*	--	0.47	0.47	0.41	0.33	0.26	0.45	0.38
MAT	0.14	--	--	0.14	0.14	0.27	0.25	0.14	0.1
Height	0.05	--	--	--	0.21	0.24	0.36	0.39	0.33
Altitude	0.04	--	--	--	--	0.24	0.38	0.38	0.35
Age	0.04	--	--	--	--	--	-0.31	-0.39	-0.38
N	0.02	--	--	--	--	--	--	0.04	0.07
LAI	0.02	--	--	--	--	--	--	--	0.21
Total $adjR^2$	--	0.23*	0.45**	0.47**	0.51**	0.55**	0.61**	0.54	0.57
<i>Urbanski Integration Method (All Sites)<sup>c</sup></i>									
cDOY	0.35**	-0.59	-0.7	-0.74	-0.67	-0.64	-0.83	-0.85	-0.85
MAP	0.23*	--	0.38	0.38	0.33	0.31	0.34	0.42	0.37
MAT	0.15	--	--	-0.06	0.06	0.06	0	0.01	-0.01
Altitude	0.05	--	--	--	0.18	0.24	0.34	0.31	0.29
Age	0.04	--	--	--	--	-0.14	-0.33	-0.33	-0.33
Height	0.03	--	--	--	--	--	0.45	0.38	0.34
N	0.02	--	--	--	--	--	--	-0.03	-0.01
LAI	0	--	--	--	--	--	--	--	0.14
Total $adjR^2$	--	0.35**	0.47**	0.48**	0.5**	0.51**	0.65***	0.69**	0.71**
<i>Dynamic Integration Method (All Sites)<sup>d</sup></i>									
cDOY	0.47***	-0.68	0.39	-0.66	-0.6	-0.58	-0.6	-0.84	-0.86
MAP	0.22*	--	-0.64	0.39	0.35	0.34	0.23	0.45	0.39
MAT	0.14	--	--	-0.04	0.06	0.05	0.06	0	-0.04
Altitude	0.06	--	--	--	0.15	0.2	0.29	0.27	0.24
Age	0.04	--	--	--	--	-0.13	-0.25	-0.31	-0.3
Height	0.02	--	--	--	--	--	0.29	0.38	0.33
N	0.02	--	--	--	--	--	--	0.01	0.03
LAI	0.01	--	--	--	--	--	--	--	0.18
Total $adjR^2$	--	0.47***	0.62**	0.62***	0.63***	0.65***	0.7***	0.72**	0.74**
<i>Dynamic Integration Method (ENF Only)<sup>e</sup></i>									
cDOY	0.58**	-0.76	-0.4	-1.03	-1.08	-1.16	-1.09	-1.04	-0.71
MAT	0.17	--	-1.07	-0.4	-0.42	-0.38	-0.36	-0.22	0.43
Age	0.13	--	--	-0.09	-0.11	-0.06	-0.04	-0.2	-0.72
LAI	0.06	--	--	--	0.35	0.2	0.23	0.15	-0.04
MAP	0.04	--	--	--	--	0.36	0.36	0.46	0.56
N	0.03	--	--	--	--	--	0	-0.1	-0.25
Height	0.01	--	--	--	--	--	--	0.22	0.71
Altitude	0.01	--	--	--	--	--	--	--	0.53
Total $adjR^2$	--	0.58**	0.65	0.66**	0.78**	0.87***	0.87**	0.88*	0.94*
<i>Dynamic Integration Method (DBF Only)<sup>f</sup></i>									
cDOY	0.68*	-0.83	0.37	-0.44	-0.4	-0.37	--	--	--
Altitude	0.53	--	-0.61	0.43	0.44	0.16	--	--	--
Age	0.33	--	--	0.23	0.22	0.29	--	--	--
LAI	0.27	--	--	--	0.07	0.24	--	--	--
MAP	0.17	--	--	--	--	0.38	--	--	--
N	0.11	--	--	--	--	--	--	--	--
MAT	0.03	--	--	--	--	--	--	--	--
Height	0.02	--	--	--	--	--	--	--	--
Total $adjR^2$	--	0.68*	0.78*	0.81*	0.81	0.86	--	--	--

<sup>a</sup>The variables were included one by one in the models (cDOY = compensation day; MAT = mean annual air temperature at the top of the eddy towers; LAI = leaf area index; Age = average age of the mature trees in the stand; Height = maximum tree height; N = mean annual nitrogen deposition; MAP = mean annual sum of precipitation). The  $\beta$  coefficients (var) indicate the relative importance of the variable, ranging from -1 (highest importance, negative correlation) to +1 (highest importance, positive correlation). The first column gives the  $R^2$  for individual site characteristics (see Table 1).

<sup>b</sup>Classical (all sites).

<sup>c</sup>Urbanski (all sites).

<sup>d</sup>Dynamic (all sites).

<sup>e</sup>The analysis for the dynamic integration for evergreen needleleaf forests (ENF) only.

<sup>f</sup>The analysis for the dynamic integration for deciduous broadleaf forests (DBF) only. Other forest types had too low replications ( $n = 3$ ) for a separate analysis.

\* $p < 0.05$ .

\*\* $p < 0.01$ .

\*\*\* $p < 0.001$ .

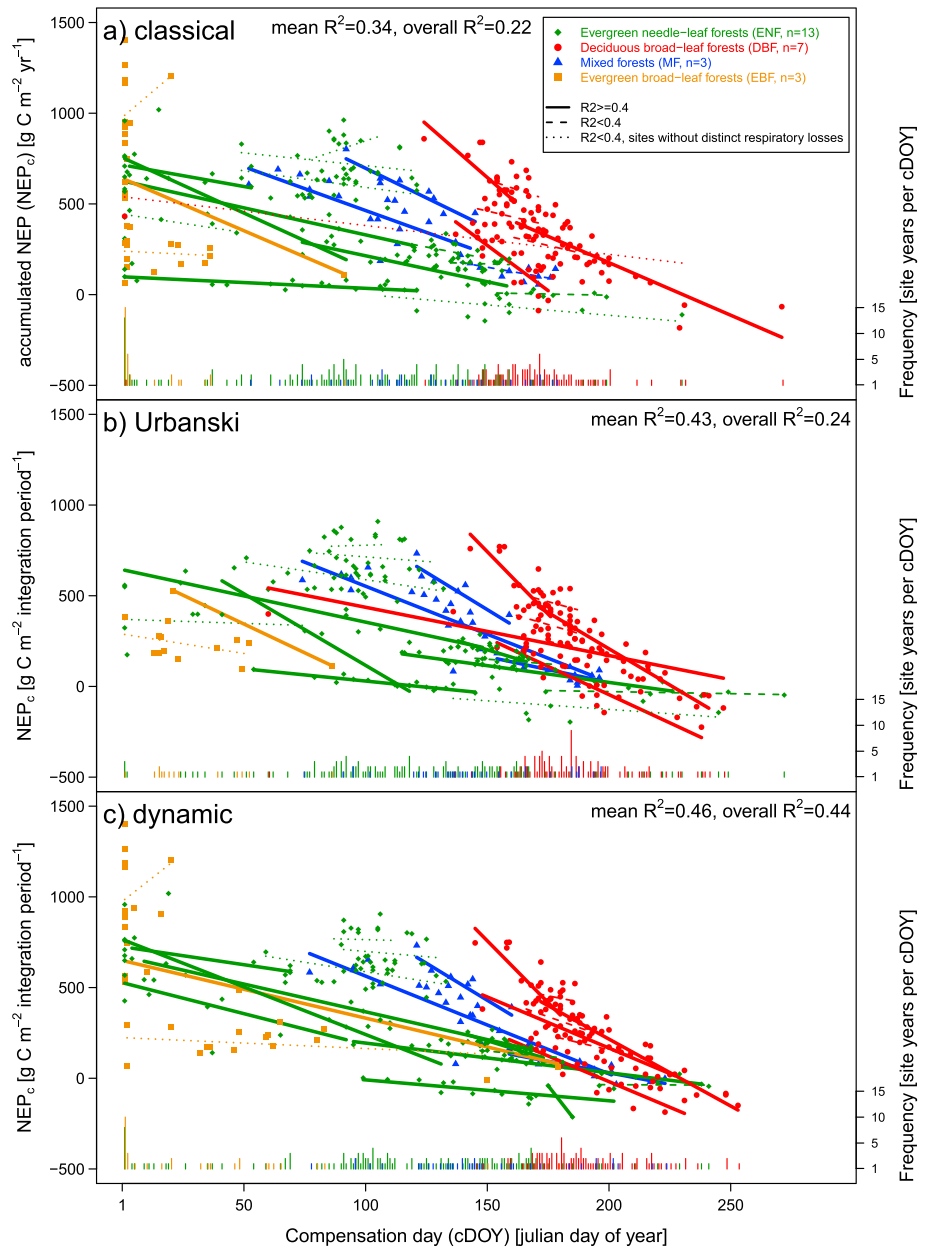


**Figure 4.** Linear regressions between compensation days (cDOY) and annual sums of net ecosystem productivity ( $NEP_c$ ) (Table 1) for each site and integration method: (a) classical, (b) Urbanski, and (c) dynamic. Solid regression lines are shown for  $R^2 \geq 0.4$ , broken lines for the rest. The frequency columns at the bottom of each panel indicate the number of site years occurring at a specific cDOY (color coded for the four forest types).

Mean annual temperature (MAT) was the secondary determinant variable of  $NEP_c$  in stepwise multiple linear regression models (Table 4). The ranking of site factors, with minor contributions, such as leaf area index (LAI), mean annual precipitation (MAP), and stand age followed next; however, the ranking depended on the integration method. An exception was the DBF sites (Table 4e): MAT had no explanatory weight for  $NEP_c$  at these sites, in line with the finding that cDOY of these forests was not determined by MAT (Figure 3).

When analyzing individual sites instead of pooled data, the site-specific relationships between cDOY and  $NEP_c$  showed a high variability and ranged from not existing to excellent (annual resolution, Table 1 and Figures 4 and 5). There appeared clear clusters of points (in the scatterplot of cDOY versus  $NEP_c$ , according

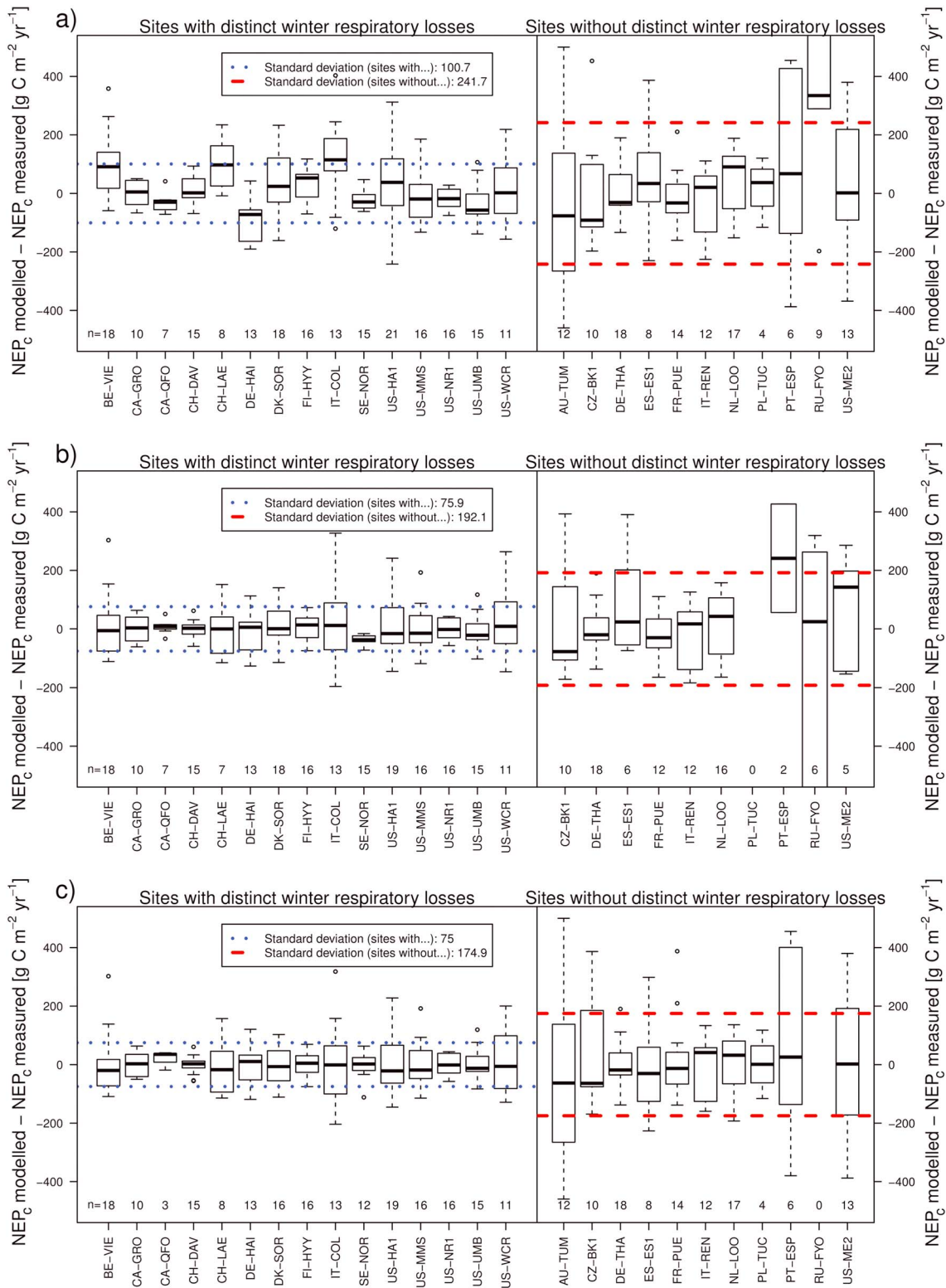


**Figure 5.** Differences between modeled annual net ecosystem productivity (NEP<sub>C</sub>), as a linear function of cDOY and measured NEP<sub>C</sub> for each site in a leave-one-year-out cross evaluation for each integration method: (a) Classical, (b) Urbanski, and (c) dynamic. The results are grouped for sites with and without distinct winter net respiratory losses. The Urbanski method was left out for AU-Tum, there, the “year” begins on 1 July and goes to 30 June one year later.

to the forest types in Figure 4): evergreen forests (ENF and EBF) had the lowest cDOY with the highest  $NEP_c$ . Deciduous broadleaf forest (DBF) had the highest cDOYs with on average lower  $NEP_c$ . Mixed forest (MF) had average cDOYs with relatively high  $NEP_c$ .

The site-specific quality of the relationships between cDOY and  $NEP_c$  was largely explicable by grouping the pooled data according to sites with and without a distinct net respiratory carbon loss over wintertime (Table 2). The separation criterion for the two groups was a net respiration loss of 10% of the annual  $NEP_c$  (Table 2). Sites with distinct winter respiration loss had on average a stronger correlation between cDOY and  $NEP_c$  ( $R^2$  0.53 versus 0.37; dynamic method) and were on average 4°C cooler than sites with no distinct winter respiration loss (Tables 1 and 2).

### 3.4. Quality of $NEP_c$ Predictions From cDOY

The quality of  $NEP_c$  predictions from cDOY were tested by comparing measured and modeled  $NEP_c$  per site and year with a leave-one-year-out cross evaluation (Figure 5). There were two very clear results: 1. The Urbanski and the dynamic integration methods led to distinctly better  $NEP_c$  prediction than the classical integration method over the Gregorian/orbital calendar year. 2. The  $NEP_c$  predictions from cDOY were stronger for sites with a distinct respiratory carbon loss over wintertime. Thereby, sites where the forest did not become a C source for a distinct period, and thus did not lose at least 10% of annual  $NEP_c$  every year, failed to show a strong prediction of  $NEP_c$  from cDOY.

## 4. Discussion

There is increasing evidence that a considerable proportion of the interannual variability of  $NEP_c$  cannot be explained by the current year's climatic variability alone but needs considering previous periods' weather factors. Predispositions of growth by the determination of buds in autumn of the past year [Thomas *et al.*, 2009; Zweifel *et al.*, 2006], carry-over effects on physiology in years following climate extremes [Law *et al.*, 2002; Thomas *et al.*, 2009; Wu *et al.*, 2012; Zielis *et al.*, 2014], C-storage pools accumulated over several years [Capioli *et al.*, 2009; Hoch *et al.*, 2003], sapwood-related hydraulic traits [Zweifel *et al.*, 2006], and winter chilling effects (vernalization) [Cook *et al.*, 2012] are examples of potential causalities between conditions back in time and the current year  $NEP_c$ . In order to better understand the intraannual variability of  $NEP_c$  and its drivers, we introduced the day of compensation (cDOY), i.e., the day of the current year (typically in spring) when net carbon losses during wintertime are compensated by carbon assimilation in spring or early summer (Figure 1). cDOY reflects the complete winter conditions and the related accumulated  $CO_2$  losses, in combination with the onset and rate of  $CO_2$  assimilation in spring (Table 2). Therefore, cDOY is not directly comparable with studies focusing on the onset of GPP or the change in  $NEP/NEE$  from a C source to a sink in spring [Delpierre *et al.*, 2009; Gonsamo *et al.*, 2012a; Gonsamo *et al.*, 2012b] since these approaches do not account for the amount of accumulated respiratory C losses over wintertime. In the following we discuss the meaning of cDOY and its impact on the interpretation of  $NEP_c$ .

### 4.1. Mean Annual Site Temperature Determining cDOY

The loss of C during wintertime and the respective cDOY was found to be statistically highly independent of most of the site characteristics like mean annual precipitation, nitrogen deposition, leaf area index, age, or tree height (Table 3). Only MAT was significantly related to cDOY ( $R^2$  about 0.4, pooled data for all sites, Table 3) particularly when the sites were grouped according to their forest types ( $R^2$  up to 0.99, Figure 3, with one exception, see below).

The importance of air and soil temperatures for the recovery of trees from the inactive physiological winter dormancy back into a physiologically active status is well documented [Baldocchi *et al.*, 2005] and covers issues such as rehydration of tissues [Koike, 1990; Lundmark *et al.*, 1988; Suni *et al.*, 2003; Zweifel *et al.*, 2000], bud burst [Basler and Körner, 2014], assimilation [Monson *et al.*, 2011a], flowering [Cook *et al.*, 2012], length of the vegetation/growth period [Aurela *et al.*, 2004; Baldocchi and Wilson, 2001; Churkina *et al.*, 2005; Monson *et al.*, 2011a], growth [Zweifel *et al.*, 2010], and probably many more. All these processes are, finally, determining cDOY with different weights, since they are influencing quantities and timing of ecosystem respiration and assimilation, explaining the influence of MAT on cDOY well.

#### 4.1.1. One Exception: The Deciduous Broadleaf Forests

There was one exception from the generally close relationship between MAT and cDOY: MAT had no impact on cDOY for deciduous broadleaf forests (DBF,  $n = 7$ ) (Figure 3), but cDOY had a high explanatory power for  $NEP_c$ , particularly with the dynamic integration method (Table 4e). This finding was unchanged when considering DBF filtering for those sites with a distinct winter respiratory carbon loss of more than 10% of the annual  $NEP_c$  (Figure 3b, negative sign = respiratory loss/positive  $NEP_c$ ). Overall, this means that cDOY is strongly forest type specific and that cDOY includes information not covered by the site characteristics investigated and thus offers a new dimension in interpreting  $NEP_c$ . This seems to be particularly true for the DBF sites. The seven DBF forests included in this study (IT-COL, US-MMS, DE-HAI, US-HA1, US-WCR, DK-SOR, and US-UMB) consisted of beech (*Fagus sylvatica*), maple (*Acer* spp.), oak (*Quercus* spp.), ash (*Fraxinus* spp.), basswood (*Tilia americana*), and sourwood trees (*Oxydendrum arboreum*). We suggest two potential explanations why the cDOY of these forests does not depend on MAT. First, (i) the group of DBF sites might still be too heterogeneous in terms of their species composition to show a concise MAT-cDOY relationship. The limited number of replications ( $n = 7$ ) for this group does, however, not allow for further differentiations. And second, (ii) cDOY reflects processes which are indeed independent of MAT for this forest type, e.g., due to biological predispositions of water and carbon storage which have their origin before the time period investigated [Keenan et al., 2012; Urbanski et al., 2007; Zielis et al., 2014; Zweifel et al., 2010], or due to genetic predispositions which determine the regulation of physiological activity independently of temperature [Basler and Körner, 2014], or in a way that positive and negative temperature effects level each other off. A convincing chain of arguments for the second explanation was recently brought up by Cook et al. [2012]. They showed that increasing temperatures during winter and spring induce opposite effects in certain species. Warmer winter conditions can lead to an insufficient vernalization, i.e., chilling requirements that must be met before a plant is able to respond to spring warming, which in turn leads to a delayed initiation of phenological processes in spring despite the positive effect of increased spring temperatures. Further, for beech trees Basler and Körner [2014] recently reported a codetermination of beech bud burst by the photoperiod and, therefore, a partial decoupling from temperature. Such a partial decoupling from temperature in terms of physiological processes could be, in terms of physiological processes, a species-specific explanation for a predisposition disturbing the generally valid relationship between MAT and cDOY. The effect of climate change on the relationship between cDOY and  $NEP$  might thus also depend on species-specific physiological responses and acclimation potentials. It is however difficult to understand how heterotrophic respiration ( $R_H$ ) in the soil is triggered by the mentioned tree physiological processes. Apart from temperature,  $R_H$  might be stimulated by rhizosphere processes such as root exudates and mycorrhiza, which in turn might be more closely coupled to the tree physiological status in DBF. Further field studies are needed to test this hypothesis.

#### 4.2. Timing of cDOY

In general, evergreen forests (EBF and ENF) had earlier cDOYs than the deciduous forests, and mixed forests with evergreen and deciduous species were in between (Figure 4). Photosynthesis of evergreens during winter varies with climatic region, but can be substantial. Thus, the early cDOYs of the evergreens may be explained by the ability of evergreen trees to start earlier in the season with assimilation [Richardson et al., 2010] or even maintain it during mild winters [Pallardy, 2010]. Photosynthetic capacity can be attained after just a few days of sufficient environmental conditions [Ottander et al., 1995; Ottander and Oquist, 1991; Suni et al., 2003].

Forest types, excepting DBF, and cDOY are both found to be linked to MAT (Figure 3 and Table 3). Evergreen broadleaf forest (EBF), for instance, grows at relatively warm sites and do not have a consistently occurring winter respiratory carbon loss period and thus show no consistently cDOY timings in each year (Figure 3). Typical examples are the eucalypt sites in Australia and Portugal (Table 2 and supporting information Figure S AU-TUM and S PT-ESP). These sites show an almost full year growth period or at least do not turn into C sources once every year, and the cDOYs, which can hardly occur, happen thus hardly any year. At the other end of the biological scale appear the deciduous broadleaf tree sites (DBF) with the latest cDOYs (Figure 4) at the generally cooler sites (Figure 3). The existence of a cold season is the main reason for forming a deciduous canopy. Deciduous forests need more time in spring for bud burst and leaf flushing, for the development of the photosynthetic apparatus, and for the onset of photosynthetic activity [Basler and



Körner, 2014; Epron *et al.*, 1996; Jurik, 1986; Koike, 1990; Reich *et al.*, 1991]. The evergreen needleleaf forests (ENF) have the widest temporal range for cDOY (Figure 4), again in line with the widest range of occurring MAT (Figure 3a).

### 4.3. Strengths and Limitations of cDOY to Predict $NEP_c$

The explanatory power of cDOY as a predictor of  $NEP_c$  was strongly depending on whether the site had a net carbon respiratory loss higher than 10% of the annual  $NEP_c$  or not (Figures 4 and 5). For sites with a distinct net carbon loss over wintertime (Figure 5a) the estimated annual  $NEP_c$  from cDOY reached accuracies of  $\pm 75 \text{ g C m}^{-2} \text{ yr}^{-1}$  which are comparable to some of the most successful (but much more complex)  $NEP$  models [Keenan *et al.*, 2012]. For the other sites without a distinct winter respiratory loss, the standard deviation between modeled and measured  $NEP_c$  was a factor 2 to 3 higher (Figure 5b), which leads to the conclusion that cDOY is of limited explanatory power in these cases. This could be explained partly by the large variation in winter photosynthesis in temperate evergreens, and by the fact that evergreen needleleaf species grow in some of the harshest conditions, such as the western U.S. where summer drought is the norm [Law and Waring, 2015].

Besides the importance of the winter net respiratory C loss, the forest type had a strong influence on the predictive power of cDOY on  $NEP_c$ . Pooled data reached an  $R^2$  of 0.47 (dynamic integration) for the linear regression between cDOY and  $NEP_c$  (Table 4), whereas the grouped data for ENF ( $R^2 = 0.58$ , dynamic integration, Table 4e) and DBF ( $R^2 = 0.68$ , dynamic integration, Table 4d) were much higher. This again indicates that the information content of cDOY, i.e., the net effect of winter and spring processes, depends on the forest type and the respective species composition (Figure 4). Both winter respiratory loss and vegetation type are related to temperature and therefore linked to each other (Figure 3). It is therefore not surprising that besides cDOY as the variable with the highest explanatory power for  $NEP_c$ , mean annual temperature appeared as the second best driver in our stepwise multiple regression analyses (Table 4). The addition of other site factors, namely precipitation, age, or LAI improved the multiple regressions further. Generally, the goodness of fit between cDOY and  $NEP_c$  increased with the timing of later cDOYs and with decreasing air temperatures (Table 4).

We conclude that lower mean annual temperatures lead to generally more pronounced winter net respiratory losses and it appears plausible that this is linked to later cDOYs. This is also in line with studies analyzing the onset of forests as a C sink in relation to winter and spring temperatures [Baldocchi *et al.*, 2005; Cook *et al.*, 2012; Delpiere *et al.*, 2009; Monson *et al.*, 2011b]. Or the other way around, the warmer the site the less distinct the carbon loss period may be the earlier cDOY happens and the less likely the influence of cDOY on annual carbon uptake. Furthermore, we conclude that latter cDOYs are linked to lower annual  $NEP_c$ , and thus, the influence of cDOY on the annual  $NEP_c$  increases with its timing.

cDOYs of deciduous broadleaf forests (DBF) showed the highest prediction quality for  $NEP_c$  (Table 4e) despite the fact that the respective cDOY did not correlate with mean annual temperature (Figure 3) nor other site variables like for other forests types (Table 4d) or the pooled data (Tables 4a–4c). Sites at higher altitudes (e.g., US-NR1 and US-Me2) experience large interannual variation in the physiological active period, for example, 45 days at US-Me2 [Thomas *et al.*, 2009], and studies in the mountains of the western U.S. have shown declining snowpack for decades and its correlation with warm temperature anomalies. Further at US-NR1, longer growing seasons were correlated with low snow water equivalent and resulted in less annual net carbon uptake [Hu *et al.*, 2010]. Overall, such processes may confound an explanatory power of MAT for cDOY and  $NEP_c$  in certain cases; however, we found no generally convincing explanation for the relationship between cDOY (its not found drivers) and  $NEP_c$ . Even when not understanding why DBF sites appear as a special case, we conclude that cDOY timing must in general depend on variables (eventually beyond the ones we analyzed) containing information about the site and its past (climatic) history, including genetic predispositions leading to this high predictive power for  $NEP_c$ .

In summary, there are many indications for winter effects on  $NEP_c$  of forests and related to it on the cDOY timing. The compensation day (cDOY) is suggested to capture air temperature and intrinsic forest type-dependent differences, leading to a specific date in the first part of the calendar year, with a high explanatory power for the upcoming annual  $NEP_c$  values of the entire year for forest sites under distinct respiratory net carbon losses during wintertime.

#### 4.4. Starting the $NEP_c$ Year in Autumn

Three different ways of integrating NEP over a year were applied: the static “classical” calendar-year method (1 January to 31 December), the static “Urbanski” method (28 October to 27 October), and the more process-oriented “dynamic” method, defining the “biological” year as the period between two annual  $NEP_c$  peaks. There appeared distinctly better fits between cDOY and  $NEP_c$  for the two methods starting the  $NEP_c$  year in autumn (Table 4). The classical method performed generally worse for all types of analyses (Tables 3 and 4 and Figure 5). The additional gain of predictive quality for the dynamic method over the static Urbanski method was relatively small. This means that it is important to include the complete autumn and winter period before the actual C sink period for interpreting  $NEP_c$ , but doing so with a static approach captures more or less the same information as when doing so with the site- and year-specific dynamic method (which can be more labor intensive to deal with).

#### 4.5. Conclusions

The compensation day cDOY reflects processes, which take place before the net C-sink period begins in forests in spring and early summer. The fact that cDOY explains more of  $NEP_c$  when starting the  $NEP_c$  year in autumn shows that the (autumn-winter) period already before 1 January plays an important role for the following  $NEP_c$  performance. cDOY analysis takes seasonal and interannual variations of the carbon cycle dynamics into account and is therefore suggested to take up carry-over effects of climate and carbon storage in temperate forests [Keenan et al., 2012; Urbanski et al., 2007; Zielis et al., 2014; Zweifel et al., 2010]. Such carry-over effects seem to be less important in forests with no distinct winter net respiratory loss of C (C loss less than 10% of annual  $NEP_c$ ). This is in line with the finding that cDOY gains explanatory power for  $NEP_c$  at sites with distinct winter respiratory C losses. The fact that biological processes, occurring before the annual net assimilation period begins, are able to explain more than 50% of the annual  $NEP_c$  should change our view on the drivers of  $NEP_c$ . Weather conditions during the main assimilation period of a forest seem to tell only half the story of the annual  $NEP_c$ . Thus, an accurate  $NEP_c$  interpretation additionally needs to include the conditions that affected a forest before this period.

#### Acknowledgments

The authors are grateful for the funding from both the Swiss National Science Foundation (grant PDFMP3\_132562) and the State Secretariat for Education, Research and Innovation (COST SBF1 C10.0101). The study was part of COST Action FP0903 “Climate Change and Forest Mitigation and Adaptation in a Polluted Environment” (MAFor). We furthermore acknowledge the funding for two COST Short-Term Scientific Missions (Action FP0903) to Sweden (Anders Lindroth, Fredrik Lagergren, and Meelis Mölder) and to Poland (Janusz Olejnik and Marek Urbaniak). This work was also supported by the Ministry of Education, Youth and Sports of CR within the National Sustainability Program I (NPU I), grant LO1415. A. Varlagin was supported by the Russian Science Foundation (Project 14-27-00065). The data used in this study have been retrieved from the FluxNet2015 data set (<http://fluxnet.fluxdata.org/data/fluxnet2015-dataset/>) or from the GHG Europe Database (<http://www.europe-fluxdata.eu/ghg-europe/guide-lines/obtaining-data/general-information>) (see Table 1), and we acknowledge the support from (alphabetically) Peter Blanken, Gil Bohrer, Carole Coursolle, Peter Curtis, Anne Deligne, Ankur Desai, Damiano Gianelle, Allen Goldstein, Richard Joffre, Tanguy Manise, Hank Margolis, Kimberly Ann Novick, Bill Munger, Dario Papale, Eva Van Gorsel, and Will Woodgate. Some sites have been funded by AmeriFlux or Fluxnet\_Canada. In addition, we are grateful for the statistical consulting by Mark Hannay from the Seminar for Statistics, ETH Zürich. Last but not least we are particularly grateful to the Editor, the Associated Editor and both reviewers for their very helpful and productive reviews.

#### References

- Aubinet, M., T. Vesala, and D. Papale (2012), *Eddy Covariance—A Practical Guide to Measurement and Data Analysis*, pp. 59–171, Springer, Netherlands.
- Aurela, M., T. Laurila, and J. Tuovinen (2004), The timing of snow melt controls the annual  $CO_2$  balance in a subarctic fen, *Geophys. Res. Lett.*, *31*, L16119, doi:10.1029/2004GL020315.
- Baldocchi, D. D., T. Black, P. Curtis, E. Falge, J. Fuentes, A. Granier, L. Gu, A. Knohl, K. Pilegaard, and H. Schmid (2005), Predicting the onset of net carbon uptake by deciduous forests with soil temperature and climate data: A synthesis of FLUXNET data, *Int. J. Biometeorol.*, *49*(6), 377–387.
- Baldocchi, D., and K. Wilson (2001), Modelling  $CO_2$  and water vapour exchange of a temperate broadleaved forest across hourly to decadal time scales, *Ecol. Modell.*, *142*, 155–184.
- Basler, D., and C. Körner (2014), Photoperiod and temperature responses of bud swelling and bud burst in four temperate forest tree species, *Tree Physiol.*, *34*(4), 377–388, doi:10.1093/treephys/tpu021.
- Beringer, J., et al. (2016), An introduction to the Australian and New Zealand flux tower network—OzFlux, *Biogeosciences Discuss.*, *13*, 5895–5916.
- Brzostek, E. R., D. Dragoni, H. P. Schmid, A. F. Rahman, D. Sims, C. A. Wayson, D. J. Johnson, and R. P. Phillips (2014), Chronic water stress reduces tree growth and the carbon sink of deciduous hardwood forests, *Global Change Biol.*, *20*(8), 2531–2539.
- Campoli, M., A. Michelsen, A. Demey, A. Vermeulen, R. Samson, and R. Lemeur (2009), Net primary production and carbon stocks for subarctic mesic-dry tundras with contrasting microtopography, altitude, and dominant species, *Ecosystems*, *12*(5), 760–776.
- Churkina, G., D. Schimel, B. H. Braswell, and X. Xiao (2005), Spatial analysis of growing season length control over net ecosystem exchange, *Global Change Biol.*, *11*(10), 1777–1787, doi:10.1111/j.1365-2486.2005.001012.x.
- Ciais, P., et al. (2005), Europe-wide reduction in primary productivity caused by the heat and drought in 2003, *Nature*, *437*(7058), 529–533, doi:10.1038/nature03972.
- European Fluxes Database Cluster (2014), Online resource: <http://www.europe-fluxdata.eu/>, last accessed on April 13, 2014.
- Cook, B. D., K. J. Davis, W. Wang, A. Desai, B. W. Berger, R. M. Teclaw, J. G. Martin, P. V. Bolstad, P. S. Bakwin, and C. Yi (2004), Carbon exchange and venting anomalies in an upland deciduous forest in northern Wisconsin, USA, *Agric. For. Meteorol.*, *126*(3), 271–295.
- Cook, B. I., E. M. Wolkovich, and C. Parmesan (2012), Divergent responses to spring and winter warming drive community level flowering trends, *Proc. Natl. Acad. Sci.*, *109*(23), 9000–9005.
- Coursolle, C., H. Margolis, M.-A. Giasson, P.-Y. Bernier, B. Amiro, M. Arain, A. Barr, T. Black, M. Goulden, and J. McCaughey (2012), Influence of stand age on the magnitude and seasonality of carbon fluxes in Canadian forests, *Agric. For. Meteorol.*, *165*, 136–148.
- Delpierre, N., K. Soudani, C. Francois, B. Köstner, J. Y. Pontailler, E. Nikinmaa, L. Misson, M. Aubinet, C. Bernhofer, and A. Granier (2009), Exceptional carbon uptake in European forests during the warm spring of 2007: A data-model analysis, *Global Change Biol.*, *15*(6), 1455–1474.
- Dragoni, D., H. P. Schmid, C. A. Wayson, H. Potter, C. S. B. Grimmond, and J. C. Randolph (2011), Evidence of increased net ecosystem productivity associated with a longer vegetated season in a deciduous forest in south-central Indiana, USA, *Global Change Biol.*, *17*(2), 886–897.

- Epron, D., R. Liozon, and M. Mousseau (1996), Effects of elevated CO<sub>2</sub> concentration on leaf characteristics and photosynthetic capacity of beech (*Fagus sylvatica*) during the growing season, *Tree Physiol.*, *16*(4), 425–432, doi:10.1093/treephys/16.4.425.
- Flechard, C. R., et al. (2011), Dry deposition of reactive nitrogen to European ecosystems: A comparison of inferential models across the NitroEurope network, *Atmos. Chem. Phys.*, *11*(6), 2703–2728, doi:10.5194/acp-11-2703-2011.
- Gökkaya, K., V. Thomas, T. Noland, H. McCaughey, and P. Treitz (2014), Testing the robustness of predictive models for chlorophyll generated from spaceborne imaging spectroscopy data for a mixed wood boreal forest canopy, *Int. J. Rem. Sens.*, *35*(1), 218–233.
- Gökkaya, K., V. Thomas, T. L. Noland, H. McCaughey, I. Morrison, and P. Treitz (2015), Prediction of macronutrients at the canopy level using spaceborne imaging spectroscopy and LiDAR data in a mixed wood boreal forest, *Rem. Sens.*, *7*(7), 9045–9069.
- Gonsamo, A., J. M. Chen, D. T. Price, W. A. Kurz, and C. Wu (2012a), Land surface phenology from optical satellite measurement and CO<sub>2</sub> eddy covariance technique, *J. Geophys. Res.*, *117*, G03032, doi:10.1029/2012JG002070.
- Gonsamo, A., J. M. Chen, C. Wu, and D. Dragoni (2012b), Predicting deciduous forest carbon uptake phenology by upscaling FLUXNET measurements using remote sensing data, *Agric. For. Meteorol.*, *165*, 127–135.
- Gough, C., C. Vogel, H. Schmid, H.-B. Su, and P. Curtis (2008), Multi-year convergence of biometric and meteorological estimates of forest carbon storage, *Agric. For. Meteorol.*, *148*(2), 158–170.
- Gough, C. M., B. S. Hardiman, L. E. Nave, G. Bohrer, K. D. Maurer, C. S. Vogel, K. J. Nadelhoffer, and P. S. Curtis (2013), Sustained carbon uptake and storage following moderate disturbance in a Great Lakes forest, *Ecol. Appl.*, *23*(5), 1202–1215.
- Grünwald, T., and C. Bernhofer (2007), A decade of carbon, water and energy flux measurements of an old spruce forest at the Anchor Station Tharandt, *Tellus B*, *59*(3), 387–396.
- Herbst, M., M. Mund, R. Tamrakar, and A. Knohl (2015), Differences in carbon uptake and water use between a managed and an unmanaged beech forest in central Germany, *For. Ecol. Manage.*, *355*, 101–108.
- Hoch, G., A. Richter, and C. Körner (2003), Non-structural carbon compounds in temperate forest trees, *Plant, Cell Environ.*, *26*(7), 1067–1081.
- Holmsgaard, E. (1955), Arranganalyser af danske skovtraeeer, *Det forstl. forogsvaesens i Danmark*, *22*(1).
- Hu, J., D. J. Moore, S. P. Burns, and R. K. Monson (2010), Longer growing seasons lead to less carbon sequestration by a subalpine forest, *Global Change Biol.*, *16*(2), 771–783.
- Jurik, T. W. (1986), Seasonal patterns of leaf photosynthetic capacity in successional northern hardwood tree species, *Am. J. Bot.*, *73*(1), 131–138, doi:10.2307/2444285.
- Keenan, T., et al. (2012), Terrestrial biosphere model performance for inter-annual variability of land-atmosphere CO<sub>2</sub> exchange, *Global Change Biol.*, *18*(6), 1971–1987, doi:10.1111/j.1365-2486.2012.02678.x.
- Keith, H., E. Van Gorsel, K. L. Jacobsen, and H. A. Cleugh (2012), Dynamics of carbon exchange in a Eucalyptus forest in response to interacting disturbance factors, *Agric. For. Meteorol.*, *153*, 67–81.
- Knohl, A., E.-D. Schulze, O. Kolle, and N. Buchmann (2003), Large carbon uptake by an unmanaged 250-year-old deciduous forest in Central Germany, *Agric. For. Meteorol.*, *118*(3), 151–167.
- Koike, T. (1990), Autumn colouring, photosynthetic performance and leaf development of deciduous broadleaved trees in relation to forest succession, *Tree Physiol.*, *7*(1–4), 21–32.
- Lagergren, F., A. Lindroth, E. Dellwik, A. Ibrom, H. Lankreijer, S. Launiainen, M. MÖlder, P. Kolari, K. I. M. Pilegaard, and T. Vesala (2008), Biophysical controls on CO<sub>2</sub> fluxes of three northern forests based on long-term eddy covariance data, *Tellus B*, *60*(2), 143–152, doi:10.1111/j.1600-0889.2006.00324.x.
- Law, B., and R. Waring (2015), Carbon implications of current and future effects of drought, fire and management on Pacific Northwest forests, *For. Ecol. Manage.*, *355*, 4–14.
- Law, B., E. Falge, L. V. Gu, D. Baldocchi, P. Bakwin, P. Berbigier, K. Davis, A. Dolman, M. Falk, and J. Fuentes (2002), Environmental controls over carbon dioxide and water vapor exchange of terrestrial vegetation, *Agric. For. Meteorol.*, *113*(1), 97–120.
- Le Maire, G., N. Delapierre, M. Jung, P. Ciais, M. Reichstein, N. Viovy, A. Granier, A. Ibrom, P. Kolari, and B. Longdoz (2010), Detecting the critical periods that underpin interannual fluctuations in the carbon balance of European forests, *J. Geophys. Res.*, *115*, G00H03, doi:10.1029/2009JG001244.
- Lundmark, T., J. Heden, and J. E. Hallgren (1988), Recovery from winter depression of photosynthesis in pine and spruce, *Trees*, *2*(2), 110–114, doi:10.1007/BF00196757.
- McCaughey, J., M. Pejam, M. Arain, and D. Cameron (2006), Carbon dioxide and energy fluxes from a boreal mixed wood forest ecosystem in Ontario, Canada, *Agric. For. Meteorol.*, *140*(1), 79–96.
- Monson, R., D. Moore, N. Trahan, L. Scott-Denton, S. Burns, J. Hu, and D. Bowling (2011a), Process coupling and control over the response of net ecosystem CO<sub>2</sub> exchange to climate variability and insect disturbance in subalpine forests of the Western US, Abstracts B13J-01 presented at 2011 Fall Meeting, AGU, San Francisco, Calif.
- Monson, R., D. Moore, N. Trahan, L. Scott-Denton, S. Burns, J. Hu, and D. Bowling (2011b), Process coupling and control over the response of net ecosystem eCO<sub>2</sub> exchange to climate variability and insect disturbance in subalpine forests of the Western US, Abstracts B13J-01 presented at 2011 Fall Meeting, AGU, San Francisco, Calif.
- Mund, M., W. Kutsch, C. Wirth, T. Kahl, A. Knohl, M. Skomarkova, and E.-D. Schulze (2010), The influence of climate and fructification on the inter-annual variability of stem growth and net primary productivity in an old-growth, mixed beech forest, *Tree Physiol.*, *30*(6), 689–704.
- Munger, J. W., S. C. Wofsy, P. S. Bakwin, S. M. Fan, M. L. Goulden, B. C. Daube, A. H. Goldstein, K. E. Moore, and D. R. Fitzjarrald (1996), Atmospheric deposition of reactive nitrogen oxides and ozone in a temperate deciduous forest and a subarctic woodland: 1. Measurements and mechanisms, *J. Geophys. Res.*, *101*, 12,639–12,657, doi:10.1029/96JD00230.
- Munger, J. W., S.-M. Fan, P. S. Bakwin, M. L. Goulden, A. Goldstein, A. S. Colman, and S. C. Wofsy (1998), Regional budgets for nitrogen oxides from continental sources: Variations of rates for oxidation and deposition with season and distance from source regions, *J. Geophys. Res.*, *103*, doi:10.1029/98JD00168.
- Nave, L. E., C. S. Vogel, C. M. Gough, and P. S. Curtis (2009), Contribution of atmospheric nitrogen deposition to net primary productivity in a northern hardwood forest, *Can. J. For. Res.*, *39*(6), 1108–1118.
- Ottander, C., and G. Oquist (1991), Recovery of photosynthesis in winter-stressed Scots pine, *Plant Cell Environ.*, *14*(3), 345–349, doi:10.1111/j.1365-3040.1991.tb01511.x.
- Ottander, C., D. Campbell, and G. Oquist (1995), Seasonal changes in photosystem II organization and pigment composition in *Pinus sylvestris*, *Planta*, *197*(1), 176–183, doi:10.1007/BF00239954.
- Pallardy, S. G. (2010), *Physiology of Woody Plants*, 3rd ed., Academic Press, San Diego, Calif.
- Pilegaard, K., A. Ibrom, M. S. Courtney, P. Hummelshøj, and N. O. Jensen (2011), Increasing net CO<sub>2</sub> uptake by a Danish beech forest during the period from 1996 to 2009, *Agric. For. Meteorol.*, *151*(7), 934–946.

- Pita, G., B. Gielen, D. Zona, A. Rodrigues, S. Rambal, I. A. Janssens, and R. Ceulemans (2013), Carbon and water vapor fluxes over four forests in two contrasting climatic zones, *Agric. For. Meteorol.*, *180*, 211–224.
- Quinn, G., and M. Keough (2002), *Experimental Design and Data Analysis for Biologists*, Cambridge Univ. Press, Cambridge.
- R Development Core Team (2013), R: A language and environment for statistical computing: <http://www.R-project.org>, Vienna, Austria: R Foundation for Statistical Computing, 1–1731.
- Reich, P. B., M. B. Walters, and D. S. Ellsworth (1991), Leaf age and season influence the relationships between leaf nitrogen, leaf mass per area and photosynthesis in maple and oak trees, *Plant Cell Environ.*, *14*(3), 251–259, doi:10.1111/j.1365-3040.1991.tb01499.x.
- Reichstein, M., et al. (2005), On the separation of net ecosystem exchange into assimilation and ecosystem respiration: Review and improved algorithm, *Global Change Biol.*, *11*(9), 1424–1439, doi:10.1111/j.1365-2486.2005.001002.x.
- Reichstein, M., et al. (2013), Climate extremes and the carbon cycle, *Nature*, *500*(7462), 287–295, doi:10.1038/nature12350.
- Richardson, A. D., D. Y. Hollinger, D. B. Dail, J. T. Lee, J. W. Munger, and J. O’Keefe (2009), Influence of spring phenology on seasonal and annual carbon balance in two contrasting New England forests, *Tree Physiol.*, *29*(3), 321–331, doi:10.1093/treephys/tpn040.
- Richardson, A. D., et al. (2010), Influence of spring and autumn phenological transitions on forest ecosystem productivity, *Philos. Trans. R. Soc. London, Ser. B*, *365*(1555), 3227–3246, doi:10.1098/rstb.2010.0102.
- Rodrigues, A., G. Pita, J. Mateus, C. Kurz-Besson, M. Casquilho, S. Cerasoli, A. Gomes, and J. Pereira (2011), Eight years of continuous carbon fluxes measurements in a Portuguese eucalypt stand under two main events: Drought and felling, *Agric. For. Meteorol.*, *151*(4), 493–507.
- Roman, D., K. Novick, E. Brzostek, D. Dragoni, F. Rahman, and R. Phillips (2015), The role of isohydric and anisohydric species in determining ecosystem-scale response to severe drought, *Oecologia*, *179*(3), 641–654.
- Scartazza, A., D. Di Baccio, P. Bertolotto, O. Gavrichkova, and G. Matteucci (2016), Investigating the European beech (*Fagus sylvatica* L.) leaf characteristics along the vertical canopy profile: Leaf structure, photosynthetic capacity, light energy dissipation and photoprotection mechanisms, *Tree Physiol.*, *36*(9), 1060–1076.
- Schmid, H. P., C. S. B. Grimmond, F. Cropley, B. Offerle, and H.-B. Su (2000), Measurements of CO<sub>2</sub> and energy fluxes over a mixed hardwood forest in the mid-western United States, *Agric. For. Meteorol.*, *103*(4), 357–374.
- Schwarz, P., B. Law, M. Williams, J. Irvine, M. Kurpius, and D. Moore (2004), Climatic versus biotic constraints on carbon and water fluxes in seasonally drought-affected ponderosa pine ecosystems, *Global Biogeochem. Cycles*, *18*, GB4007, doi:10.1029/2004GB002234.
- Shao, J., X. Zhou, Y. Luo, B. Li, M. Aurela, D. Billesbach, P. D. Blanken, R. Bracho, J. Chen, and M. Fischer (2016), Direct and indirect effects of climatic variations on the interannual variability in net ecosystem exchange across terrestrial ecosystems, *Tellus B*, *68*, 30,575.
- Sievering, H., T. Kelly, G. McConville, C. Seibold, and A. Turnipseed (2001), Nitric acid dry deposition to conifer forests: Niwot Ridge spruce–fir–pine study, *Atmos. Environ.*, *35*(22), 3851–3859.
- Suni, T., F. Berninger, T. Vesala, T. Markkanen, P. Hari, A. Mäkelä, H. Ilvesniemi, H. Hänninen, E. Nikinmaa, and T. Huttula (2003), Air temperature triggers the recovery of evergreen boreal forest photosynthesis in spring, *Global Change Biol.*, *9*(10), 1410–1426.
- Thomas, C. K., B. E. Law, J. Irvine, J. G. Martin, J. C. Pettijohn, and K. J. Davis (2009), Seasonal hydrology explains interannual and seasonal variation in carbon and water exchange in a semiarid mature ponderosa pine forest in central Oregon, *J. Geophys. Res.*, *114*, G04006, doi:10.1029/2009JG001010.
- Urbanski, S., C. Barford, S. Wofsy, C. Kucharik, E. Pyle, J. Budney, K. McKain, D. Fitzjarrald, M. Czikowsky, and J. Munger (2007), Factors controlling CO<sub>2</sub> exchange on time scales from hourly to decadal at Harvard Forest, *J. Geophys. Res.*, *112*, G02020, doi:10.1029/2006JG000293.
- Wolf, S., W. Eugster, C. Ammann, M. Hani, S. Zielis, R. Hiller, J. Stieger, D. Imer, L. Merbold, and N. Buchmann (2013), Contrasting response of grassland versus forest carbon and water fluxes to spring drought in Switzerland, *Environ. Res. Lett.*, *8*(3), 035007, doi:10.1088/1748-9326/8/3/035007.
- Wu, C., et al. (2013), Inter-annual variability of net ecosystem productivity in forests is explained by carbon flux phenology in autumn, *Global Ecol. Biogeogr.*, *22*, 994–1006.
- Wu, J., L. van der Linden, G. Lasslop, N. Carvalhais, K. Pilegaard, C. Beier, and A. Ibrom (2012), Effects of climate variability and functional changes on the inter-annual variation of the carbon balance in a temperate deciduous forest, *Biogeosciences*, *9*(1), 13–28.
- Zielis, S., S. Etzold, R. Zweifel, W. Eugster, M. Haeni, and N. Buchmann (2014), NEP of a Swiss subalpine forest is significantly driven not only by current but also by previous year’s weather, *Biogeosciences*, *11*, 1627–1635.
- Zweifel, R., and R. Hasler (2000), Frost-induced reversible shrinkage of bark of mature subalpine conifers, *Agric. For. Meteorol.*, *102*(4), 213–222, doi:10.1016/S0168-1923(00)00135-0.
- Zweifel, R., H. Item, and R. Hasler (2000), Stem radius changes and their relation to stored water in stems of young Norway spruce trees, *Trees-Struct. Funct.*, *15*(1), 50–57, doi:10.1007/s004680000072.
- Zweifel, R., L. Zimmermann, F. Zeugin, and D. M. Newbery (2006), Intra-annual radial growth and water relations of trees: Implications towards a growth mechanism, *J. Exp. Bot.*, *57*(6), 1445–1459, doi:10.1093/jxb/erj125.
- Zweifel, R., W. Eugster, S. Etzold, M. Dobbertin, N. Buchmann, and R. Hasler (2010), Link between continuous stem radius changes and net ecosystem productivity of a subalpine Norway spruce forest in the Swiss Alps, *New Phytol.*, *187*(3), 819–830, doi:10.1111/j.1469-8137.2010.03301.x.